QUO OXYGEN SENSOR: LINEAR AND NON-LINEAR FILTERING APPROACHES TO NOISE REDUCTION

C. T. Flanagan M.S.
Department of Bioengineering, University of Utah, Salt Lake City, Utah

ABSTRACT

A system for measurement of oxygen consumption (VO_2) and determination of respiratory quotient (RQ: RQ = VO_2/VCO_2) is currently being developed by a joint project between Novametrix Inc. (Wallingford CT) and the University of Utah Department of BioEngineering. The system may prove to be highly useful on extended duration space flight to monitor the metabolic rate of astronauts. The system employs a novel oxygen partial pressure sensor based on oxygen luminescence quenching technology for real-time measurement of respiratory oxygen concentration. This paper addresses the sensors's signal vs. noise properties. The signal to noise (S/N) ratio of the sensor has been found to degrade progressively with increasing oxygen partial pressure (pO_2) with the degradation appearing to become problematic at oxygen partial pressures above approximately 60%. In order to improve the (high pO_2) S/N ratio of the sensor, a number of signal processing techniques were investigated. These techniques were selected based on a qualitative assessment of the sensor's unique signal processing requirements and the effectiveness of the techniques was quantitatively characterized for comparison purposes. The techniques included linear as well as non-linear filtering strategies. The linear filtering strategies investigated consisted of two classes of notch filters while the more disparate non-linear filters consisted of classes of polynomial (Voltera series) filters, median and median-related filters, order statistic filters, morphological filters and weighted majority with minimum range filters. Each of the filters investigated were optimized using actual sensor data to improve sensor S/N ratio performance while maintaining adequate sensor dynamics. A number of candidate filters with varying degrees of computational complexity and noise suppression effectiveness are proposed for the sensor. Future studies will evaluate the performance of these filters within the framework of candidate oxygen consumption algorithms.

Key Words: Signal Processing, Filter, Indirect Calorimetry, Voltera Series, Median Filter, Order Statistic Filter, Morphological Filter, Weighted Majority with Minimum Range Filter.

Introduction

A sensor for measurement of respiratory gas based on oxygen's unique ability to quench the phosphorescent decay of a lumiphore was previously described[1]. This paper addresses the sensors's signal vs. noise properties, specifically, a number of signal processing techniques aimed at increasing the signal to noise (S/N) ratio of the sensor are investigated.

The QUO oxygen sensor's S/N ratio degrades progressively with increasing oxygen partial pressure of the gas mixture being measured. This degradation is due an increase in the peak-to-peak noise magnitude seen at higher pO_2. Table 1. shows the magnitude of the noise for steady state input increasing with pO_2. The exact point at which this S/N ratio degradation becomes problematic for any given oxygen consumption algorithm is a matter of subjectivity relative to its ultimate effect on the algorithm's accuracy. However, the author states

without proof that it is intuitively obvious that reduced S/N ratios will lead to reduced oxygen consumption algorithm accuracy regardless of the algorithm strategy employed. Thus, general improvements in S/N ratio performance are sought in this paper independent of, and preliminary to, oxygen consumption algorithm development and validation.

Table 1. Degradation of S/N ratio with increasing pO_2.

pO_2	Peak to Peak Noise Value
20%	~0.2 cmH_2O
40%	~0.3 cmH_2O
60%	~0.5 cmH_2O
80%	~0.9 cmH_2O
100%	~1.5 cmH_2O

The Signal processing strategies employed in this paper, must be optimized for a number of subjective design goals including:

- Maintenance of adequate system dynamics
- Sufficient suppression of noise at high pO_2.
- Acceptable degradation of signal at low pO_2.
- Acceptable computational complexity.

This subjectivity implies an infinite number of solutions given the continuum of possible weights for each subjective measure above. Therefore, only one weight for each subjective measure of performance is used producing only one optimal solution for each signal processing strategy employed.

Preliminaries

Linear filtering techniques exploit discernable spectral differences in signals to attenuate one signal relative to another. The type of attenuation sought (e.g. bandpass, highpass, lowpass filter) is contingent upon design goals. In order to determine what type of attenuation or filtering might be beneficial in this case, a power spectral density plot of both signals as well as noise propagating through the sensor are required.

Spectral Characterizations via Mathematical Model

The exact characteristics of the sensor, although previously modeled[2], cannot be known with certainty. Therefore a mathematical representation of the sensor to assess noise and signal propagation through the sensor might lead to inaccuracies resulting from inaccuracies in the model itself. Thus, a purely mathematical approach to signal/noise spectral characterization was not taken here.

Spectral Characterizations via Actual Sensor

The approach to signal/noise spectral characterization taken consisted of using the actual oxygen sensor, thus eliminating any possible modeling errors. Two input signals to the sensor were used. First, a DC input (unchanging pO_2) was selected such that the output variations in the sensor were assumed to be heavily influenced by noise propagation. Second, a rapidly changing binary input sequence (flat spectrum pseudo-random binary sequence) was selected such that the output of the sensor was proportionately more heavily influenced by signal propagation. The output of the sensor, given each of these input signals was then used to generate power spectral density plots which could be considered reflective of 1) the noise and 2) the signal. These plots are shown in Figure 4. of Appendix A.

Spectral Ambiguity

The plots in Figure 4. clearly indicate a large amount of spectral overlap between the sensor and the noise. Further, the overlap occurs at frequencies which characteristic of typical power spectra of human breathing. This spectral overlap significantly complicates the filtering task by calling into question the possible effectiveness of the spectral discrimination properties of linear filters as a solution methodology. *Therefore, this paper explores not only linear filters, but non-linear filters as well.*

Methods

LINEAR SIGNAL PROCESSING

Linear signal processing methods were utilized even though a clear spectral overlap exists between the sensor signal and the noise signal. The linear signal processing strategy used was a notch filter optimized to the noise power spectrum peak at approximately 2 Hz. A notch filter, also known as a bandstop filter, is a filter which contains deep notches in its frequency response characteristic which tends to null out or attenuate a certain frequency (or frequency band)[3].

The notch filter can be described in digital signal processing terms as consisting of a complex conjugate pair of zeros on or near the z-domain unit circle which creates a null at a frequency ω_o as follows:

$$z_{1,2} = e^{+/-j\omega_o} \quad (1)$$

Thus, the system function for this sensor would be defined as:

$$H(z) = ao*(1 - e^{j\omega_o})*(1 - e^{-j\omega_o}) \quad (2)$$

This type of system function, typically referred to as a finite-duration impulse response (FIR) system function, produces a notch filter which has a relatively broad bandwidth. The implications of this large bandwidth are that frequencies near but not at the frequency which we seek to attenuate may themselves become attenuated more than the desired amount. To reduce the attenuation bandwidth, a pair

of complex conjugate poles may be placed near the unit circle at the same null frequency ω_o as follows:

$$p_{1,2} = re^{+/-j\omega_o};\ r < 1 \quad (3)$$

These poles introduce a resonance at the null frequency and reduce the bandwidth of the notch filter. Introduction of the poles into the system function gives:

$$H(z) = a_o*(1-e^{j\omega o})*(1-e^{-j\omega o})/\ (1-re^{j\omega o})*(1-re^{-j\omega o}) \quad (4)$$

Which is equivalent to:

$$H(z) = a_o*(1-2*\cos\omega o*z^{-1} + z^{-2})/\ (1-2r*\cos\omega o*z^{-1} + r^2z^{-2}) \quad (5)$$

This type of system function is typically referred to as an infinite-duration impulse response (IIR) system function. The adjustable parameters in this IIR notch filter are the null frequency ω_o, a weighting coefficient a_o, and the distance from the center of the unit circle to the pole r. The system function in Equation (5) is a first order realization of a notch filter. Increasing the order of the notch filter can result in a filter with a still narrower bandwidth, this however, at the cost of increased computational complexity. Higher order notch filters can be realized by adding pairs of complex conjugate zeros and poles to the system function in Equation (5).

A number of design methods are available for IIR notch filters to determine the values of ω_o, a_o, and r, or equivalently stated to find the location of the poles and zeros. These include Chebyshev Type 1 (equiripple behavoir in passband and monotonic characteristic in stopband), Chebyshev Type 2 (monotonic in passband and equiripple in stopband) and Butterworth (magnitude response that is maximally flat in passband and monotonic overall). All of these design techniques lend themselves to particular signal processing tasks/requirements, however, this paper will abandon these commonly used techniques in favor of a design method based on the minimization of a cost function. This algorithm (described later in this paper) will seek out the pole/zero locations of an optimal filter given a particular data set. A variant of this cost function algorithm will be used in the design of all of the filters in this paper.

NON-LINEAR SIGNAL PROCESSING

An exploration of non-linear filtering strategies offered the possibility of the realization of filters which perform better than linear filters for this particular application. A study of possible non-linear techniques which might prove effective led to the following five general classes of non-linear filters for investigation:

- Polynomial (Voltera) Filters
- Median and Median-Related Filters
- Order Statistic Filters
- Morphological Filters
- Weighted Majority with Minimum Range Filters

Polynomial (Voltera) Filters

General Filtering Strategy

The approach taken to develop a Voltera series filter for the QUO sensor consisted of two steps. First, a non-linear system identification was performed using a Voltera series representation of the sensor. Second, input was be generated for both the system identification model as well as for the actual sensor. The output of the system identification model and the output of the sensor were compared. The difference consisting of noise and modeling error residuals. An adaptive second order Voltera kernel was then found by using a gradient descent search algorithm. This adaptively determined kernel has the function of transforming actual sensor output to idealized sensor output as represented by the model (Figure 1). The adaptive Voltera filter kernel was "locked" after the completion of a sufficiently long adaptation process. The "locked" kernel was then used as the kernel of a Voltera Series filter to reduce noise in the output of the sensor.

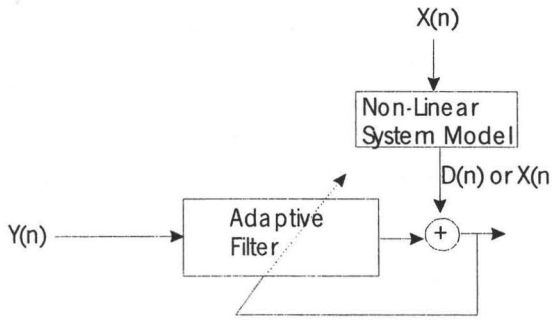

Figure 1. Adaptive Filtering Strategy Employed.

Description of Voltera Series Expansions

Recent work by V.J. Mathews[4] provides a basis for the description of non-linear systems and filters using

polynomial signal processing techniques based on Voltera series expansions.

A Voltera series expansion description of a non-linear system with memory can be expressed by the following equation:

$$y(t)=ho+\int_{-\infty}^{\infty} h1(\tau)(x(t-\tau 1)d\tau 1+\int_{-\infty}^{\infty}\int_{-\infty}^{\infty} h2(\tau 1,\tau 2)x(t-\tau 1)x(t-\tau 2)d\tau 1 d\tau 2+..$$

$$\int_{-\infty}^{\infty}....\int_{-\infty}^{\infty} hp(\tau 1...\tau p)x(t-\tau 1)..x(t-\tau p)d\tau 1..d\tau p+.... \quad (6)$$

The multidimensional functions $hp(\tau 1 \ldots \tau p)$ are called Voltera kernels and completely characterize the system much as an impulse response signal $h(\tau)$ characterizes a linear time-invariant system in the following convolution integral:

$$y(t) = \int_{-\infty}^{\infty} h(\tau)x(t-\tau)d\tau \quad (7)$$

The lower limits of integration in equation (6) are set to zero, thus limiting our discussion to causal signals or signals in which the output can only respond to changes in the input which proceed it in time. The multidimensional convolution integrals in equation (5) can be written in more compact form as:

$$\bar{h}p[x(t)\} = \int_{-\infty}^{\infty}.....\int_{-\infty}^{\infty} hp(\tau 1,....\tau p)x(t-\tau 1)..(x(t-\tau p)d\tau 1...d\tau \quad (8)$$

Thus, the Voltera series expansion can be written more compactly as:

$$y(t) = ho + \sum_{p=1}^{\infty} \overline{hp\ [x(t)]} \quad (9)$$

Where the parameter P is called the order or the degree of the Voltera series expansion.

Equations (8) and (9) can be modified to describe discrete, time-invariant, causal systems with memory as follows:

$$y(n) = ho + \sum_{p=1}^{\infty} \bar{h}p[x(n)] \quad (10)$$

$$\bar{h}p[x(n)] = \sum_{m1=0}^{\infty}...\sum_{mp=0}^{\infty} hp(m1,....,mp)x(n-m1)...x(n-mp) \quad (11)$$

where h_o is an offset term, and $h_1(m_1)$ is the impulse response of a discrete-time LTI filter and $h_p(m_1..m_p)$ is a p^{th} order impulse response which characterizes the non-linear behavior of the system. The upper limit of the summation is the amount of memory the system is assumed to have, which is our case is limited to 7 cycles which is enough memory to encapsulate the significant components of the sensor's impulse response[2].

The input-output relationship of the oxygen sensor is assumed to be second order as increasing the order beyond this will lead to filter realizations which are computationally unwieldy. Thus, given a second order model, the sensor's input-output relationship can described as follows:

$$y(n) = \Sigma a_k x(n-k) + \Sigma b_k x(n-k) + \Sigma b_k x^2(n-k) + \varepsilon(n) \quad (12)$$

Where y(n) is the system output, x(n) is the system input and $\varepsilon(n)$ is additive white noise, statistically independent of the input signal.

Voltera Kernel Determination

The Voltera kernel representation of the system, and the adaptive Voltera kernel representation of the noise (and modeling error residuals) are determined using two different methods. The Voltera kernel representation of the system is determined in "batch" mode using a least squares parameter estimation technique which is based on a minimization of the following cost function:

$$J(M) = \frac{1}{M}\sum_{k=1}^{M}(d(k) - X'(k)\bar{H})^2 \quad (13)$$

Where J(M) is the cost function which is minimized, M represents the number of samples taken, d represents the desired solution, X' represents the transpose of the input vector, and H represents the Voltera kernel. This cost function minimization problem can be shown[4] to reduce to the following easily utilized relations:

$$\bar{H}\,opt = \hat{R}_{xx}^{-1}\hat{P}_{dx} \quad (14)$$

Where $\hat{H}_{opt}$ represents the optimal Voltera kernel given $\hat{R}_{xx}^{-1}$ which represents the inverse of the autocorrelation matrix of the data and $\hat{P}_{dx}$ which represents the cross correlation vector of d(n) as follows:

$$\hat{R}_{xx} = \frac{1}{M}\sum_{k=1}^{M} X(k)X'(k) \quad (15)$$

$$\hat{P}dx = \frac{1}{M}\sum_{k=1}^{M} d(k)X(k) \quad (16)$$

The adaptive Voltera kernel for removal of noise is determined differently. An adaptive LMS approach is taken in which the idealized kernel is iteratively approached using a gradient descent search method. This algorithm is shown below:

$$\bar{H}_1(n+1) = \bar{H}_1(n) + \alpha X_1(n)e(n) \qquad (17)$$

Where α represents a small step size and e(n) represents the error vector determined as follows:

$$e(n) = d(n) - X_1'(n)\bar{H}_1(n) \qquad (18)$$

given an α small enough so as not to cause instability in the solution and large enough to ensure timely convergence, this algorithm will eventually approach the idealized solution.

Voltera Filter Hardware System

The input-output data from the sensor used in the linear filter determination in which a binary input was employed cannot be used for characterization of non-linear systems of order two and higher. In order to accurately characterize a second order non-linearity in a system, three input states must be used[5]. Thus, in order to determine the Voltera kernel of a second order system, hardware capable of generating the appropriate 3-state (trinary) input sequence, and measuring the output of the sensor was constructed. This hardware system consisted of four sub-systems (Figure 2). The first sub-system being an IBM compatible computer running a custom software program developed in the Borland C++ Builder development environment. This sub-system served to both generate trinary excitation signals as well as to

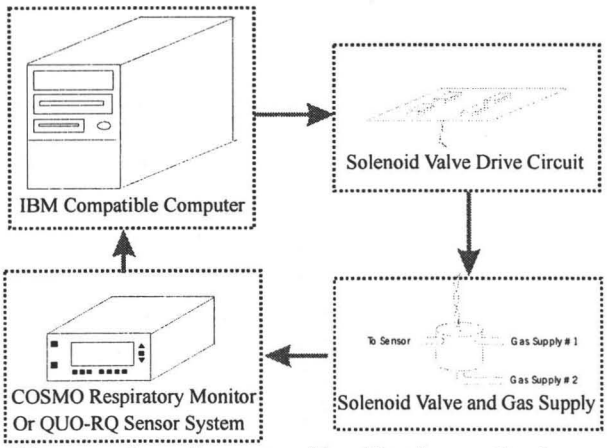

Figure 2. System identification Hardware

collect data. The excitation signals were transmitted to the solenoid valve drive circuit sub-system where the signals were amplified. The amplified excitation signals were then fed to the solenoid valve and gas supply sub-system which served to divert gas flows based on the state of the excitation signal. Finally, the oxygen sensor fed its output back to the IBM personal computer where data was collected for off-line analysis of sensor dynamics. A more detailed description of this system is contained in Reference 2.

Voltera Filter Software System

The software system used was a modified version of the software system used for linear system identification[2]. This software performs four primary tasks as follows:

- The synthesis of appropriate excitation signals
- Collection of sensor output data
- Output of random trinary sequences
- Output of data to external text file

The software is described in more detail in reference 2 and will not, in the interest of brevity, be covered here.

Median and Median-Related Filters

J.W. Tukey[6] is credited with first describing the median filter in the 1970's. Since then the non-linear median filter has been a commonly used filtering methodology in signal processing. There are a number of variants on the median filter[7], three of which were investigated for this application. These include:

- The Median Filter
- The (r,s)-Fold Trimmed Median Filter
- The Modified Trimmed Median Filter

All three strategies have at their heart, the replacement of the current signal value with a median value based on a preceding window of signal values. For example, given the following set (5 element window) of signal values:

$$\vec{x} = \{5\ 4\ 8\ 9\ 3\}$$

The median value takes the center value of ordering (e.g. MED($\vec{x}$) = {3 4 5 8 9} = 5). The median filter so named here uses this strategy and allows for variable length windows which provides some

flexibility as to the filter form. The (r,s)-Fold Trimmed Median Filter also uses this strategy but removes the r smallest and s largest values from consideration before performing the median operation. Finally, the modified trimmed median filter selects values from the window which are within a predefined value q (± q) of the median, sums those values, and divides by the number of summed values to obtain the output. The (r,s)-fold trimmed median filter allows for adjustment of r, s and window length to obtain an optimal filter and the modified trimmed median filter allows adjustment of q and window length. Thus, both the (r,s)-fold trimmed and modified median filters provide for more variation in filter morphology than the median filter.

Order Statistic Filters

This class of non-linear filters uses linear combinations of order statistics. The order statistic filter used here is referred to as the L-Filter[7]. The L-Filter performs an ordering operation on a window of data (as in median filtering) and weights each of the ordered elements according to a pre-defined coefficient vector. For instance, given the 5-element signal set:

$$\vec{x} = \{5\ 4\ 8\ 9\ 3\}$$

Further, given our coefficient vector $\bar{}$:

$$\bar{} = \{0.4\ 0.1\ 0\ 0.1\ 0.4\}$$

We have the following:

$$L\{5\ 4\ 8\ 9\ 3\} = 0.4*3 + 0.1*4 + 0*5 + 0.1*8 + 0.4*9$$
$$L\{5\ 4\ 8\ 9\ 3\} = 6.0$$

Thus, the L-Filter can be thought of as a combination of a discrete linear FIR filter and a median filter. Adjustable filter parameters include the window length and the values of the coefficient vector[§§].

Morphological Filters

The mathematic roots of morphological filters can be traced to the work of Matheron[8] and Serra[9]. These non-linear filters derive their function from the morphologic transformation of signals by sets. Starting with a mathematic description of the general morphology of a signal, these filters can remove specific undesirable shapes or contours from the signal, ideally transforming the signal into a general contour more characteristic of the true or expected Morphological filters use two basic operations called signal. This signal processing strategy can be used to great effect to remove specific undesirable features from the signal.

Dilation and *Erosion.*

These operations are related and can be considered conceptually as inverses of each other. In dilation, a moving vector (also known as a structuring element) of predefined weights (e.g. $\bar{w}(-1) = 1$, $\bar{w}(0) = 2$, $\bar{w}(1) = 1$, $\bar{w}(2) = 0$) is added to the current position in the signal set, and the maximum of these values is taken. This maximum then replaces the current value of the signal set (Y) as follows:

Signal Set Y = { 0 4 2 1 8 2 1 4 }
Y Dilated by $\bar{w}$: { - 6 8 9 10 9 - - }

Conversely, erosion takes the minimum value of the signal set Y when each element is added to the vector of weights $\bar{w}$. Thus, for erosion we obtain the following:

Signal Set Y = { 0 4 2 1 8 2 1 4 }
Y Eroded by $\bar{w}$: { - 1 2 2 1 2 - - }

A few final concepts need to be presented before proceeding to a global examination of the algorithm. First, being the concept of a symmetric structuring element set. The symmetric structuring set is obtained by rotating the original structuring set by 180 degrees in the plane:

$$\bar{w}^{s} = \{-x: x_{\in} \bar{w}\} \qquad (20)$$

Thus, given the structuring element set $\bar{w}$ already defined, we have:

$$\bar{w}(-1) = 1,\ \bar{w}(0) = 2,\ \bar{w}(1) = 1,\ \bar{w}(2) = 0$$
$$\bar{w}^{s}(-2) = 0,\ \bar{w}^{s}(-1) = 1,\ \bar{w}^{s}(0) = 2,\ \bar{w}^{s}(1) = 1$$

A sequential operation involving the erosion of a signal set by a structuring element and subsequent dilation of the eroded signal set by the symmetric

§§ The following restriction is generally placed on the coefficient vector:

$$\sum_{i=1}^{i=WindowLength} A(i) = 1 \qquad (19)$$

structuring set is known as *opening*. Conversely, a sequential operation involving the dilation of a signal set by a structuring element and subsequent erosion of the dilated signal set by the symmetric structuring set is known as *closing*. An opening operation can be conceptually understood as a rolling ball transformation[7] in which the contour followed by the rolling ball traces out the output of the filter (Figure 3). This serves to remove positive moving impulsive signal changes while broadening negative impulses. The closing operation can be pictured as the inverse, namely removing negative moving impulsive signal changes while broadening positive impulses.

The opening and closing operations can be sequentially implemented on a signal to remove particular noise shapes (as defined in the structuring element). This paper uses sequential opening and closing operations, and adjusts the structuring element values and lengths to minimize a cost function.

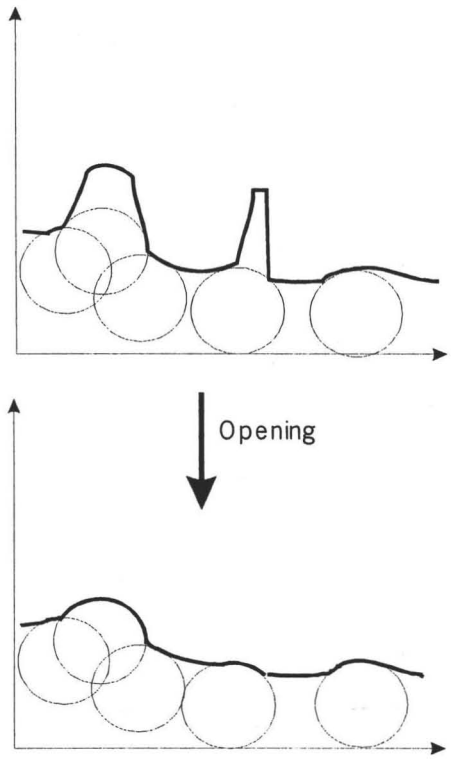

Figure 3. Rolling ball transformation (adapted from Astola and Kuosmanen[xx])

Weighted Majority with Minimum Range Filters

The weighted majority with minimum range class of filters[7] were developed with the goal of preserving high frequency signal components while attenuating noise in regions where the underlying signal is not rapidly changing. The algorithm has at its root the trimming of undesirable data. The trimming is performed to select the best concentration of the data. The algorithm uses a moving window of data selected from, and in synchrony with the progression of the signal data ($\vec{X}$). These data are then arranged using a sorting algorithm from smallest to largest value and placed in a second vector ($\vec{Y}$). An integer value m is selected such that m is less than the window length. The values of $\vec{Y}$(i+m-1) - $\vec{Y}$(i) are determined sequentially within the window. The value of $\vec{Y}$(i*) which minimizes this sequence is then chosen as a starting point in which $\vec{Y}$(i*), $\vec{Y}$(i*+1), ... $\vec{Y}$(i*+m) are multiplied by a weighting coefficient vector $\vec{A}$[§§] which itself contains m values. The weighed values are then summed and divided by m to find their arithmetic mean. This algorithm is shown numerically below for m = 3 and $\vec{A}$ = {0.6 0.3 0.1}:

i	1	2	3	4	5	6	7
$\vec{X}$	{2	1	5	6	3	4	2}
$\vec{Y}$	{1	2	2	3	4	5	6}
$\vec{Y}$(i+m-1) - $\vec{Y}$(i)	{**1**	**1**	2	2	2		}

So indices 1 and 2 minimize the range. Therefore these indices are equivalently used as a starting point for multiplication by the weighting vector $\vec{A}$:

$$= \frac{(0.6*1 + 0.3*2 + 0.1*2) + (0.6*2 + 0.3*2 + 0.2*3)}{2}$$

$$= 1.9$$

In order to optimize this filter to a particular signal data set, the values of the vector $\vec{A}$ must be chosen as well as the window length and the value of m.

GENERAL OPTIMIZATION TECHNIQUE

A number of different filtering methodologies are investigated in this paper. However, all filtering strategies are optimized to the same data set using the same optimization strategy. The optimization consists of changing filter parameters and determining a minimum mean squared error (MMSE) between an ideal signal and the actual signal. A balancing act or engineering tradeoff exists between preserving step response and attenuating the noise. Thus, two signals

were used for optimization. Optimizing for one signal attenuates noise, optimizing for the other signal preserves the dynamics of the sensor. A cost function based on these MMSE values and the number of filter related processor operations was developed for optimization. The coefficients of the cost function can be adjusted so emphasize improved step performance, improved noise attenuation and reduced algorithm complexity. In this way, the results of all of the filters can be quantitatively compared relative to their affect on sensor dynamics and relative to the degree of computational complexity of the given filter algorithm Further, the results of the filtering operations can be quantitatively compared using a S/N ratio index. All optimizations were performed in Matlab Version 6.0 (with the signal processing and system identification toolboxes installed).

Results

The results of optimizing each of the filters presented here can be seen in Figures 5 and 6 in Appendix B. These results clearly show that, after filter optimization, some filters outperform other filters specific to the data set investigated. The first plot in Figures 5 and 6 contain the (unfiltered) noise and step response as

Table 3. Subjective Ranking of Most Promising Filters

Rank	Filter	Cost Function Value	
		Noise	Step
1st	Notch Filter	0.243	1.65
2nd	L-Filter	0.18	1.73
3rd	Morphological Filter	0.88	5.12
--	Median Filter	1.50	0.87
--	(r,s)-Trimmed Median Filter	0.38	1.99
--	Modified Trimmed Median Filter	0.60	1.04
--	Weighted Median Filter	3.06	1.84
--	Weighted Majority with Minimum Range Filter	1.73	2.87
--	Voltera Filter	0.69	4.61

measured in the sensor. The plots which follow show the resulting noise and step response of the data after having been passed through the optimized filter indicated in the title of the plots. Finally, the last plot in Figures 5 and 6 provides a quantitative comparison of the MMSE values of noise and step response error. Table 2. lists the optimized filter parameters for each of the filters investigated. Table 3. Provides a subjective ranking of the most promising filtering strategies for the QUO sensor with the linear notch filter being the best candidate filter and the non-linear L-Filter being the second most promising filter. Table 4. lists the optimized filter coefficients.

Table 4. Optimized Filter Coefficients

Filter	Optimized Filter Coefficients
Notch Filter	a_o = 0.4; r = 0.94; w_o = 4.72
Morphological Filter	Closing_1 = 0.3; Closing_2 = 0.1; Closing_3 = 0.1; Closing_4 = 0.1; Closing_5 = 0.3; Opening_1 = 0.4; Opening _2 = 0.4; Opening _3 = 0.4; Opening _4 = 0.4; Opening _5 = 0.4;

L-Filter	a_1 = 0.03; a_2 = 0.03;
	a_3 = 0.06; a_4 = 0.1;
	a_5 = 0.2; a_6 = 0.2667;
	a_7 = 0.3

Median Filter	W = 7
(r,s)-Trimmed Median Filter	R = 1; s = 1; W = 8;
Modified Trimmed Median Filter	N=21; q = 1.2

Weighted Median Filter	a_1 = 0.01; a_2 = 0.01;
	a_3 = 0.02; a_4 = 0.6;
	a_5 = 3.4; a_6 = 0.6;
	a_7 = 0.02

Weighted Majority with Minimum Range Filter	A_1 = 0.8; a_2 = 0.06; a_3 = 0.06; a_4 = 0.06
Voltera Filter	V_C(1) = 9.82; V_C(2) = 4.29; V_C(3) = 3.14; V_C(4) = 1.01; V_C(5) = -3.26;V_C(6) = -6.61; V_C(7) = -7.30;V_C(8) = 2.74; V_C(9) = -1.63;V_C(10) = -1.52; V_C(11) = -1.12;V_C(12) = -0.26; V_C(13) = 1.62; V_C(14) = 3.17; V_C(15) = 3.40; V_C(16) = 4.43; Input Vector: X(n) = [x(n) x(n-1) x(n-2) x(n-3) x(n-4) x(n-5) x(n-6) x(n-7) x^2(n) x^2(n-1) x^2(n-2) x^2(n-3) x^2(n-4) x^2(n-5) x^2(n-6) x^2(n-7)]

Adaptability of Results Given Sensor Production Variability

The QUO sensor remains in a stage of development in which improvements or changes can be made to

the sensor. These future changes have the potential of affecting the results presented here. For this reason, the tools used for tuning and qualitative/quantitative assessment of filter performance have been developed to allow for relative ease of use with regards to any potential future filter retuning efforts.

Scaling of Filter Output to Expected Noise Magnitude

Table 1. indicates that noise propagating though the sensor becomes more pronounced at higher pO_2 levels. Thus, the need for filtering becomes more acute as the level of pO_2 rises. Figure 7 in Appendix C shows typical noise peak-to-peak values as plotted relative to pO_2 level. An exponential curve was fit to this data and provides a good fit ($R^2 = 0.99$). This curve will provide a basis for the weighting of filtered output given specific pO_2 input levels. This weighting is independent of the filtering methodology ultimately selected as it is simply takes the form of an exponential scaling operation on the filtered output. Further, the weighting of the filter can be adjusted by a coefficient term (k) to tune the overall filter strength:

$$\text{Noise} \propto e^{2.564*pO_2} \quad (21)$$

Thus, relative filter strength (S) should be scaled as proportional to this same expression:

$$S \propto e^{2.564*pO_2} \quad (22)$$

An adjustment coefficient (k) should be added to allow for global filter weighting as follows:

$$S \propto k*e^{2.564*pO_2} \quad \text{(for all } S < 1\text{)} \quad (23)$$

Finally, the filter strength term operates on the filter output as follows to adjust the filter output for both the exponential noise vs. pO2 curve, as well as for global filter weighting (O_{final} = Final Output Value):

$$O_{final} = (\ (\text{Unfiltered Output})*(1-S) + (\text{Filter Output})*(S)\ )\ /2$$

Additional modifications of filter output may be indicated specific to the filter chosen. For example the Notch filter magnitude may need to be adjusted relative to filtering strength to accommodate the reduced step response magnitude resulting from the filtering operation (Figure 6.)

Validation of Filtering Technique

The candidate filters will, in the future, be assessed for efficacy in candidate VO_2 algorithms. Adjustment of the global filtering weighting coefficient (k) will allow for different strengths of promising filters to be used. All filters will ultimately be judged by their performance with respect to VO_2 algorithm accuracy.

References

1. Flanagan CT: A novel oxigraphy system based on oxygen luminescence quenching. Proceedings NASA Space Grant Consortium. 1999. Salt Lake City, Utah.
2. Flanagan CT: System Identification of the QUO-RQ and COSMO+ Sensors. White paper, available through the department of BioEngineering, University of Utah. 2000. Salt Lake City, Utah.
3. Proakis J, Manolakis D: Digital Signal Processing, Principles, Algorithms, and Applications. 343-344. Prentice Hall. New Jersey. 1996.
4. Mathews, VJ.Polynomial Signal Processing. Wiley& Sons. New York. 2000.
5. Nowak R, Van Veen B: Random and Pseudorandom Inputs for Volterra Filter Identification. IEEE Trans on Signal Processing, 1994; 42:8:2124-2135.
6. Tukey JW: Exploratory Data Analysis, Addison-Wesley, Reading, MA, 1977 (1970-71: Preliminary edition).
7. Astola J, Kuosmanen P: Fundamentals of Non-Linear Digital Filering. CRC Press. New York. 1997.
8. Matheron P: Random Sets and Integral Geometry. Wiley. New York. 1975
9. Serra J: Image analysis and Mathematical Morphology. Academic Press. London. 1982.

Appendix A

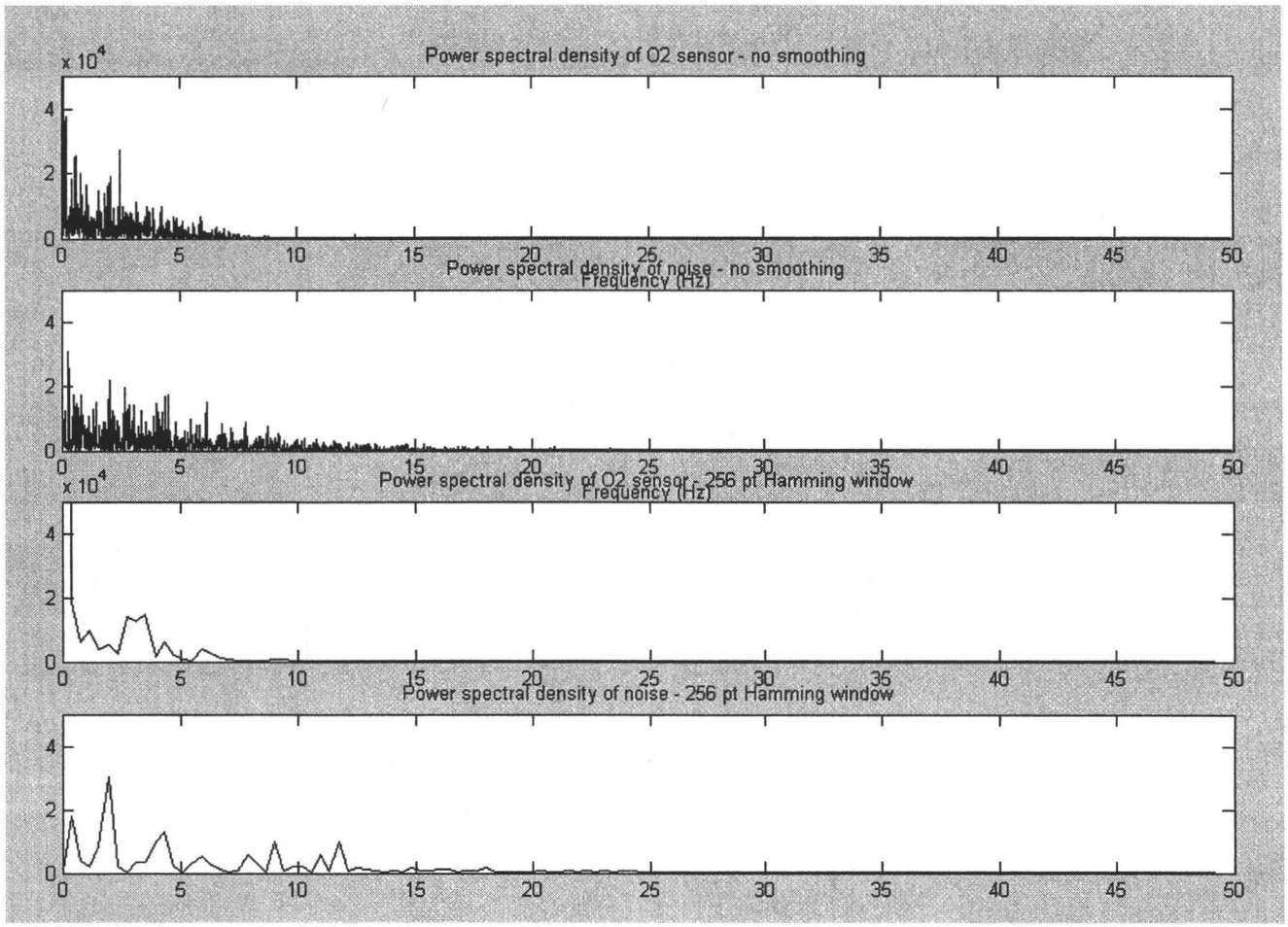

Figure 4. Power Spectral Density of Signal and Noise (Before and After application of 256 point Hamming Window)

Appendix B

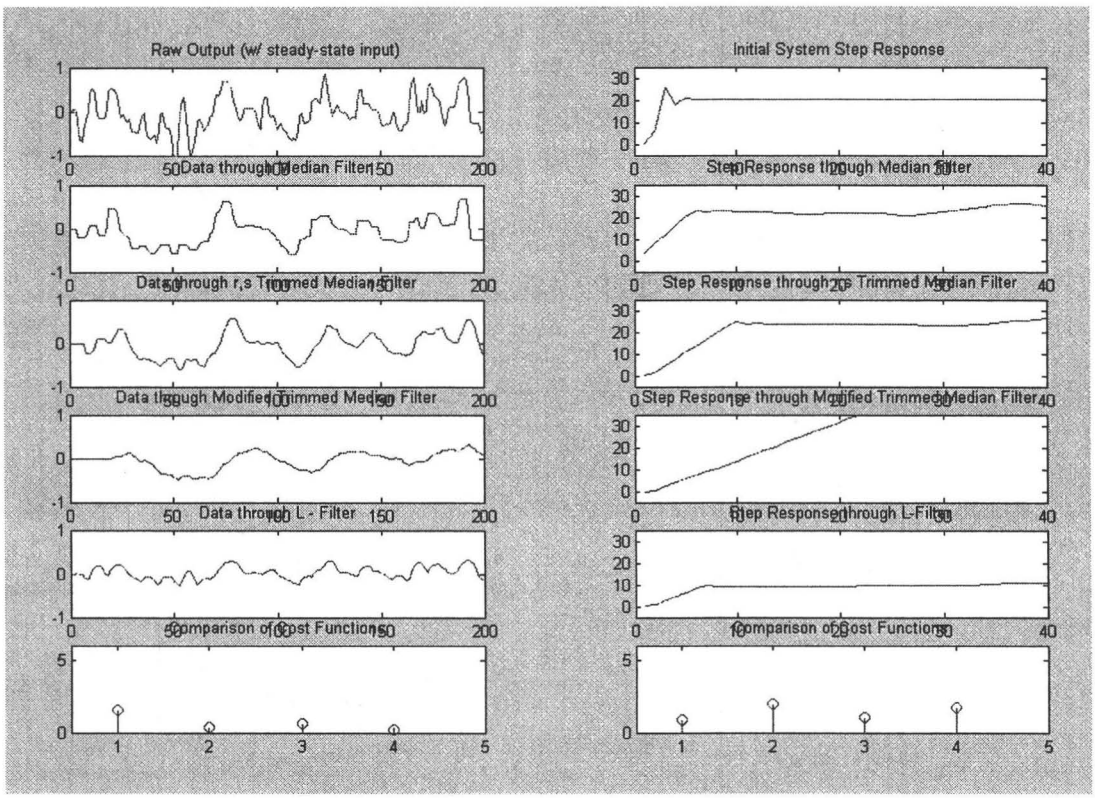

Figure 5. Raw Signal (Noise and Step) on first row. Filters investigated shown in Rows 2- 4. Tabulated cost functions in Row 5.

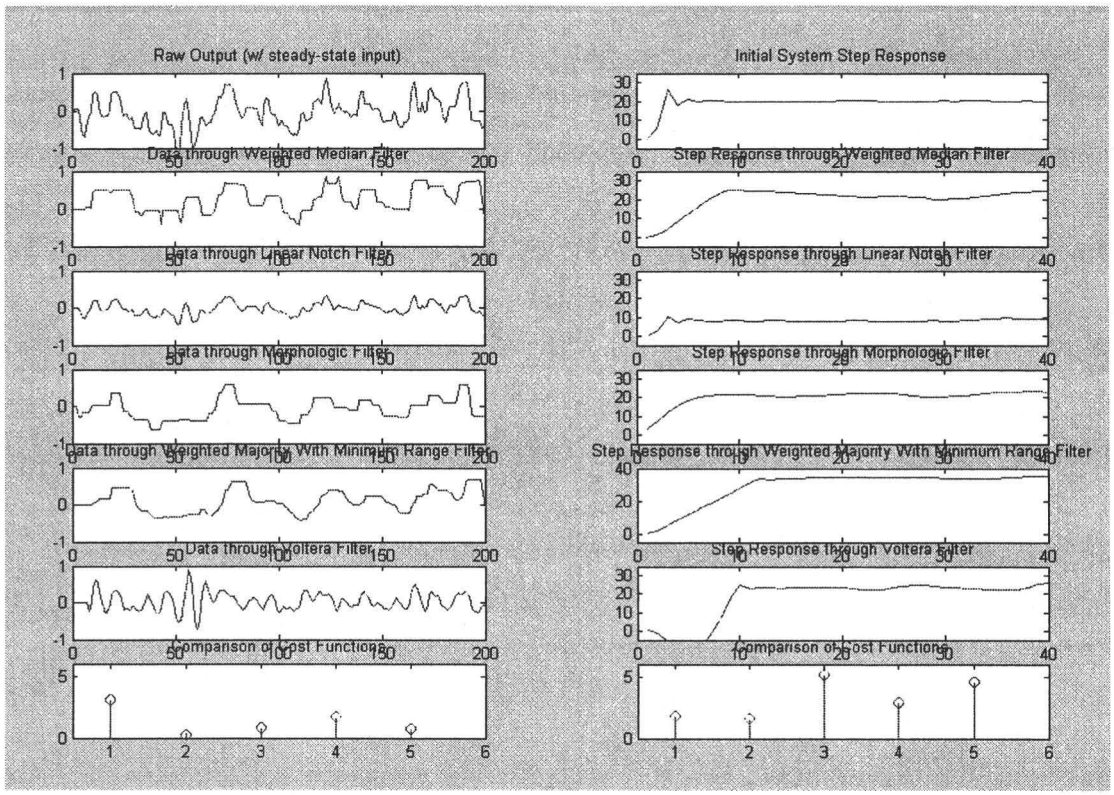

Figure 6. Raw Signal (Noise and Step) on first row. Filters investigated shown in Rows 2-5. Tabulated cost functions in Row 6.

Appendix C

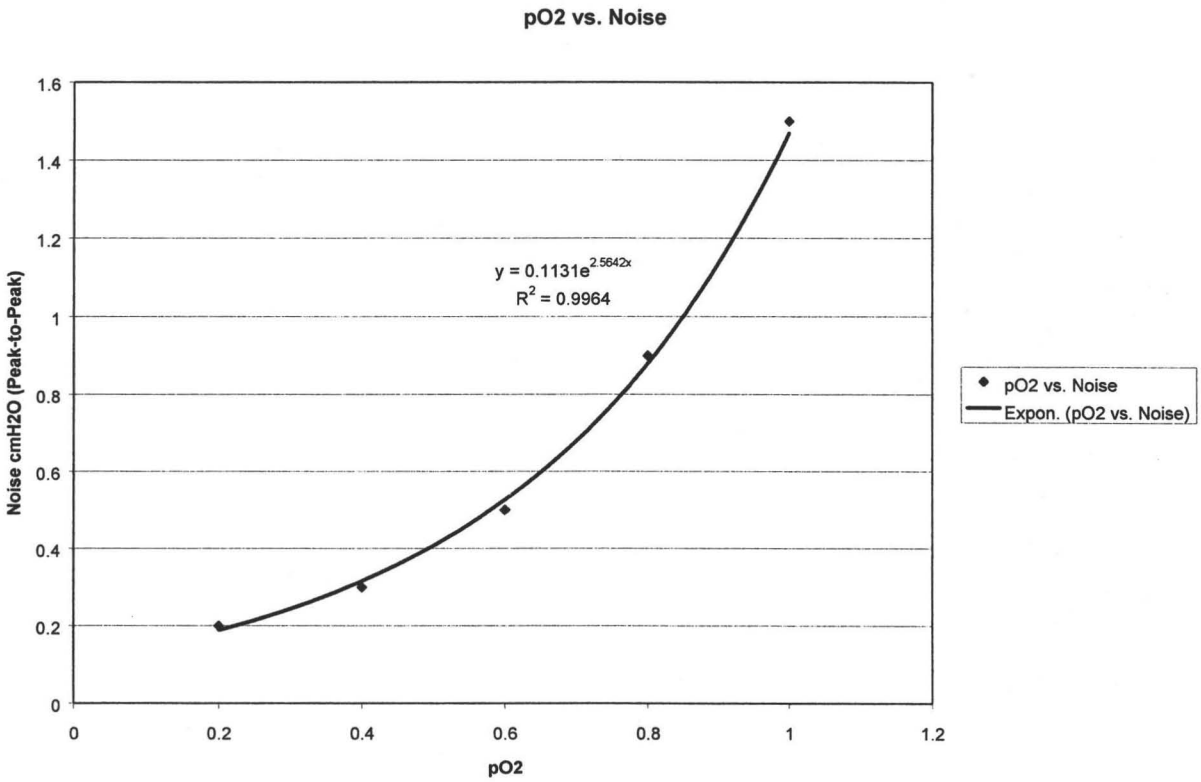

Figure 7. Noise vs. pO2 curve with exponential regression fit.